WISCONSIN UNIVERSITY OF WISCONSIN–MADISON | U.S. DEPARTMENT of ENERGY | Manufacturing Innovation Network • MIN Laboratory | Argonne NATIONAL LABORATORY

IMECE 2025-173318

High-Resolution Characterization of Machining-Induced Residual stress In Single-Crystal Sapphire

Rui Liang*, Rui Liu**, Tao Zhou**, Sangkee Min* (PI)
*University of Wisconsin-Madison, Department of Mechanical Engineering, ** Argonne National Lab, Center for Nanoscale Material

ASME SETTING THE STANDARD | NSF

IMECE Track 19-021
NSF Research Poster Competition

Project Objectives and Goals

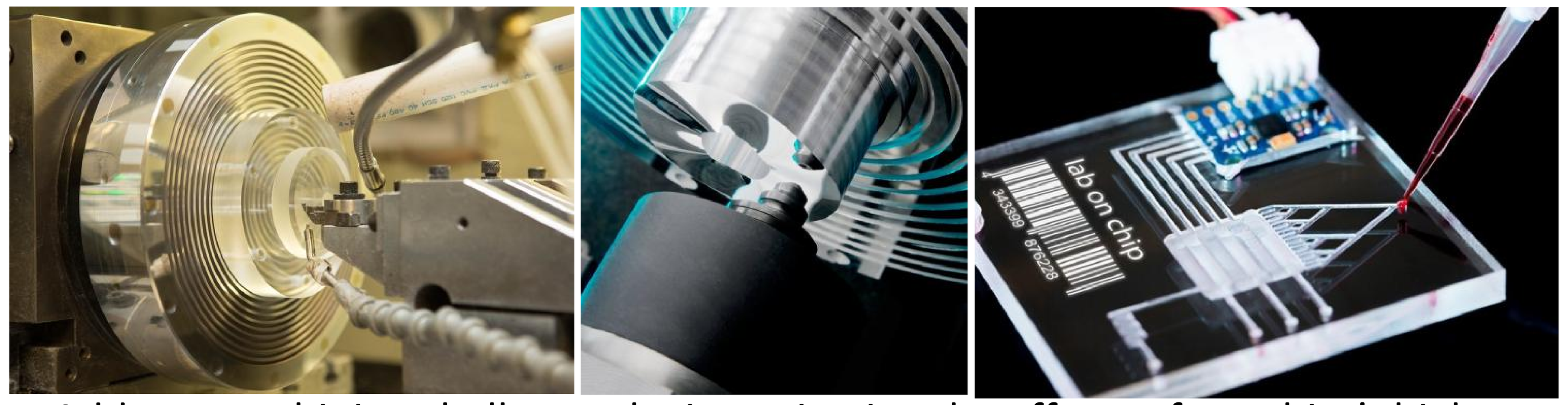

- Address machining challenges by investigating the effects of sapphire's high hardness, brittleness, and crystallographic anisotropy on material removal
- Quantify residual stress and that contribute to crack initiation and degradation of machining performance
- Utilize Raman spectroscopy to evaluate residual stress providing insights for process modeling and optimization
- Employ X-ray nanobeam diffraction microscopy, enabling high-resolution correlation between deformation mechanisms and stress evolution

Background

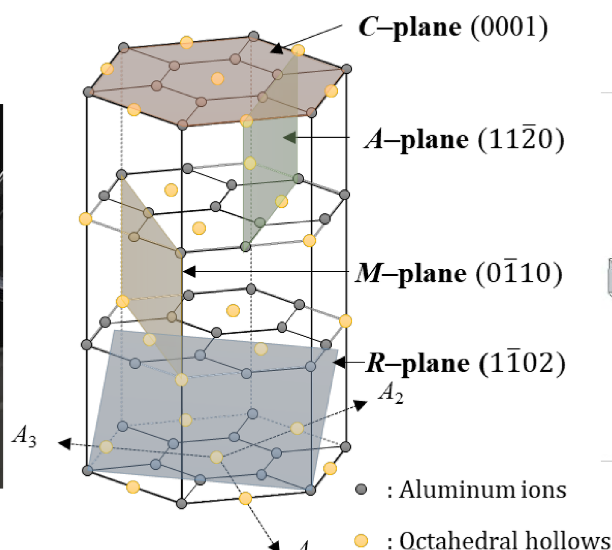

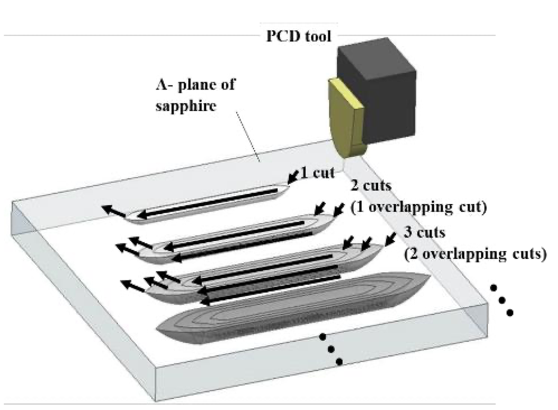

Schematic of Overlapping Cutting

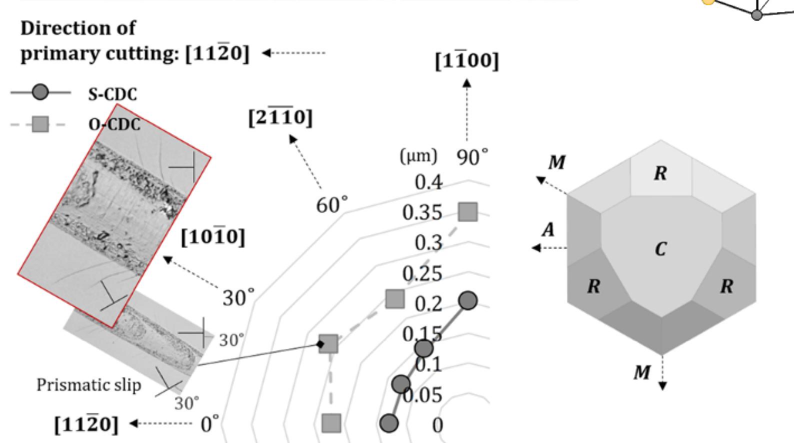

Variation in Critical Depth of Cut for Primary (O-CDC) and Subsequent Cutting (S-CDC)

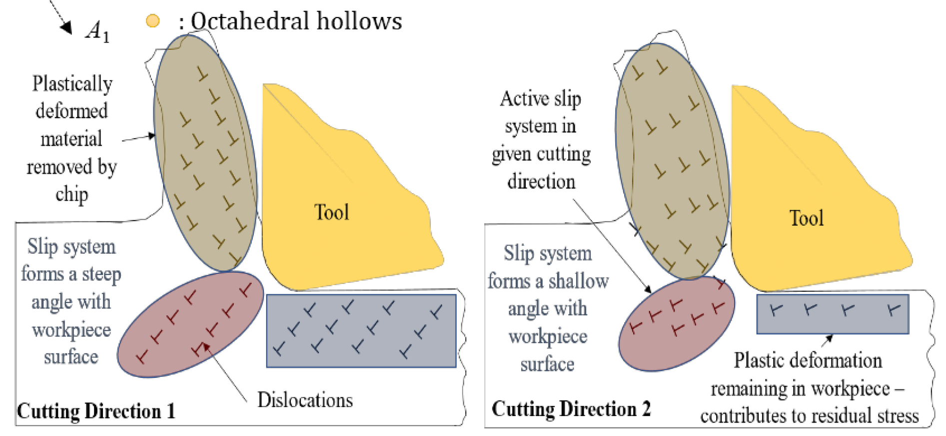

Hypothesis Correlating Residual Stress Magnitude with Plastic Deformation Mechanism

Experimental Setup

Ultra-Precision Machining Setup and Parameters

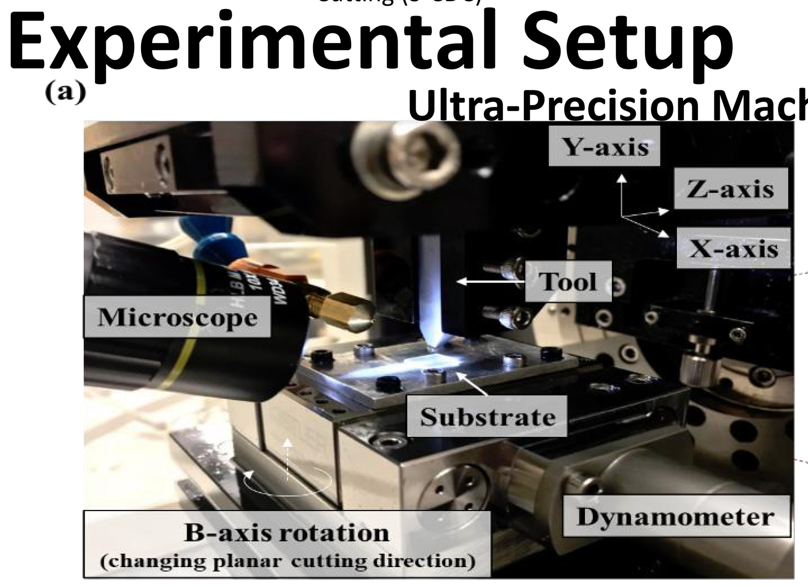

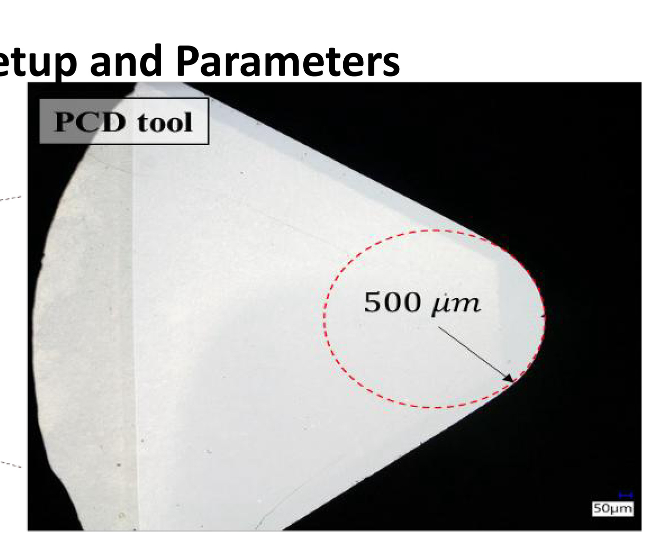

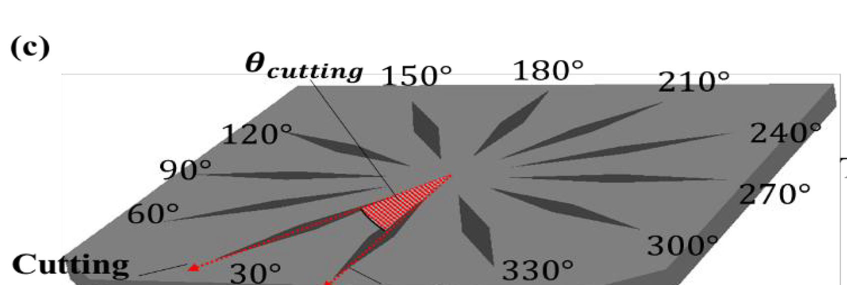

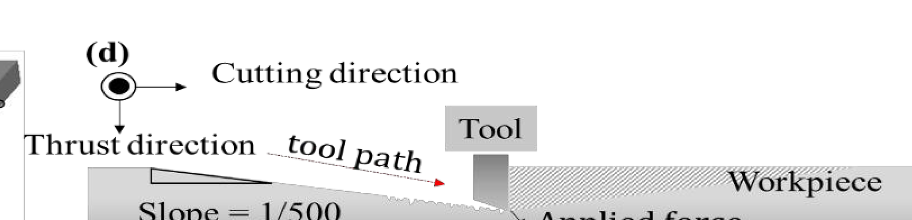

Parameter	Description
Machine Tool	ROBONANO α-0*i*B, FANUC Corp., Japan
Cutting Tool	Binderless Nano-PCD Tool, 500 µm nose radius, 0° rake angle (A.L.M.T. Corp., Japan)
Substrate	Sapphire, Czochralski growth; 3 mm x 5 mm x 0.5 mm (MTI Corp., U.S.A)
Dynamometer	Type 9119AA1 (Kistler Instrument Corp., Switzerland)
Cutting oil	Mineral oil based (JX Nippon Oil & Energy, Japan)
Feed rate	5 mm/min

Data and Results—Raman Spectroscopy

Raman Spectroscopy Parameter

Parameter	Description
Raman Instrument and Model	Horiba LabRAM HR Evolution
Laser Wavelength	633 nm
Grating Density	1800 grooves/mm
Spectral Acquisition Time	10 s/position, 2 scans per spot
Raman map spacing	~10 µm intervals

Modelling Plastic Deformation In Sapphire

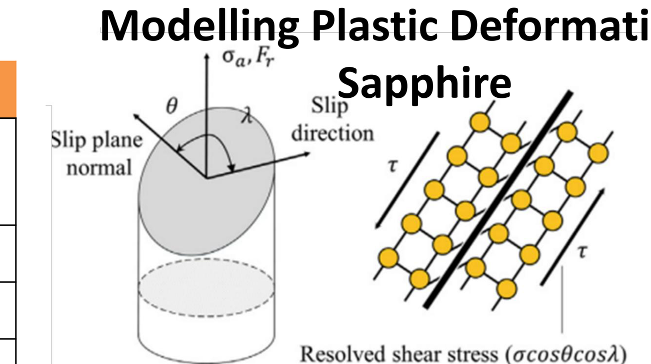

$$P_i = m_i/(\tau_i^{Crit}/min_i\tau_i^{Crit})$$

$$m_i = cos\theta_i cos\lambda_i$$

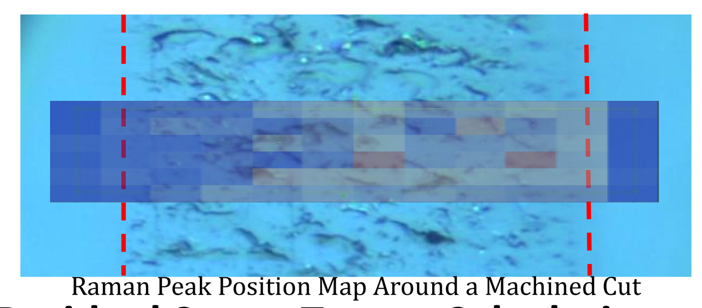
Raman Peak Position Map Around a Machined Cut

P_i: Plastic deformation parameter
m_i: Schmid factor
τ_i^{Crit}: Critical resolved shear stress
θ_i: The angle between the direction of applied stress and normal to the slip plane
λ_i: The angle between direction of applied stress and slip direction

Residual Stress Tensor Calculation

Based on the relationship between peak shift (Δv) and stress tensor(σ_{ij})

$$\Delta v = \Pi_{ij}\sigma_{ij} = \begin{vmatrix} \Pi_{11} & \Pi_{12} & \Pi_{13} \\ \Pi_{21} & \Pi_{22} & \Pi_{23} \\ \Pi_{31} & \Pi_{32} & \Pi_{33} \end{vmatrix} \begin{vmatrix} \sigma_{xx} & \sigma_{xy} & \sigma_{xz} \\ \sigma_{yx} & \sigma_{yy} & \sigma_{yz} \\ \sigma_{zx} & \sigma_{zy} & \sigma_{zz} \end{vmatrix} \quad (1)$$

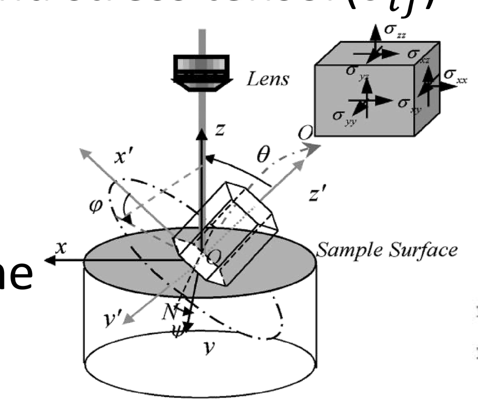

Π_{ij} is the piezo spectroscopic coefficient

Accounting for the crystal orientation in the lab frame

$$\begin{vmatrix} \sigma_{x'x'} & \sigma_{x'y'} & \sigma_{x'z'} \\ \sigma_{y'x'} & \sigma_{y'y'} & \sigma_{y'z'} \\ \sigma_{z'x'} & \sigma_{z'y'} & \sigma_{z'z'} \end{vmatrix} = \Phi_{xyz} \begin{vmatrix} \sigma_{xx} & \sigma_{xy} & \sigma_{xz} \\ \sigma_{yx} & \sigma_{yy} & \sigma_{yz} \\ \sigma_{zx} & \sigma_{zy} & \sigma_{zz} \end{vmatrix} \tilde{\Phi}_{xyz} \quad (2)$$

Φ_{xyz} is rotation matrix and $\tilde{\Phi}_{xyz}$ is the transpose of the rotation matrix.

Considering the crystal symmetries of sapphire, Eq. 1 reduces to

$$\Delta v = \begin{vmatrix} \Pi_a^{(n)} & 0 & 0 \\ 0 & \Pi_b^{(n)} & 0 \\ 0 & 0 & \Pi_c^{(n)} \end{vmatrix} \Phi_{xyz} \begin{vmatrix} \sigma_{xx} & \sigma_{xy} & \sigma_{xz} \\ \sigma_{yx} & \sigma_{yy} & \sigma_{yz} \\ \sigma_{zx} & \sigma_{zy} & \sigma_{zz} \end{vmatrix} \tilde{\Phi}_{xyz} \quad (3)$$

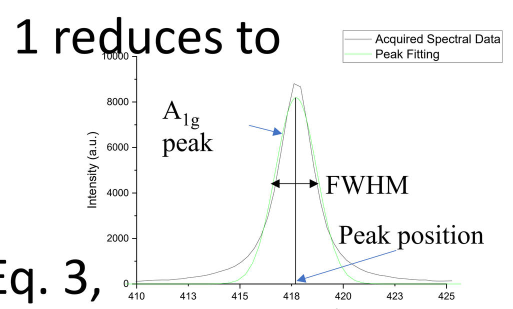

A_{1g} Phonon Peak in Sapphire

Reducing to plane strain condition and simplifying Eq. 3,

$$\begin{pmatrix} \sigma_{xx} \\ \sigma_{xy} \\ \sigma_{yy} \end{pmatrix} = \begin{pmatrix} A_{11} & A_{12} & A_{13} \\ A_{21} & A_{22} & A_{23} \\ A_{31} & A_{32} & A_{33} \end{pmatrix}^{-1} \begin{pmatrix} \Delta v_1 \\ \Delta v_2 \\ \Delta v_3 \end{pmatrix} \quad (4)$$

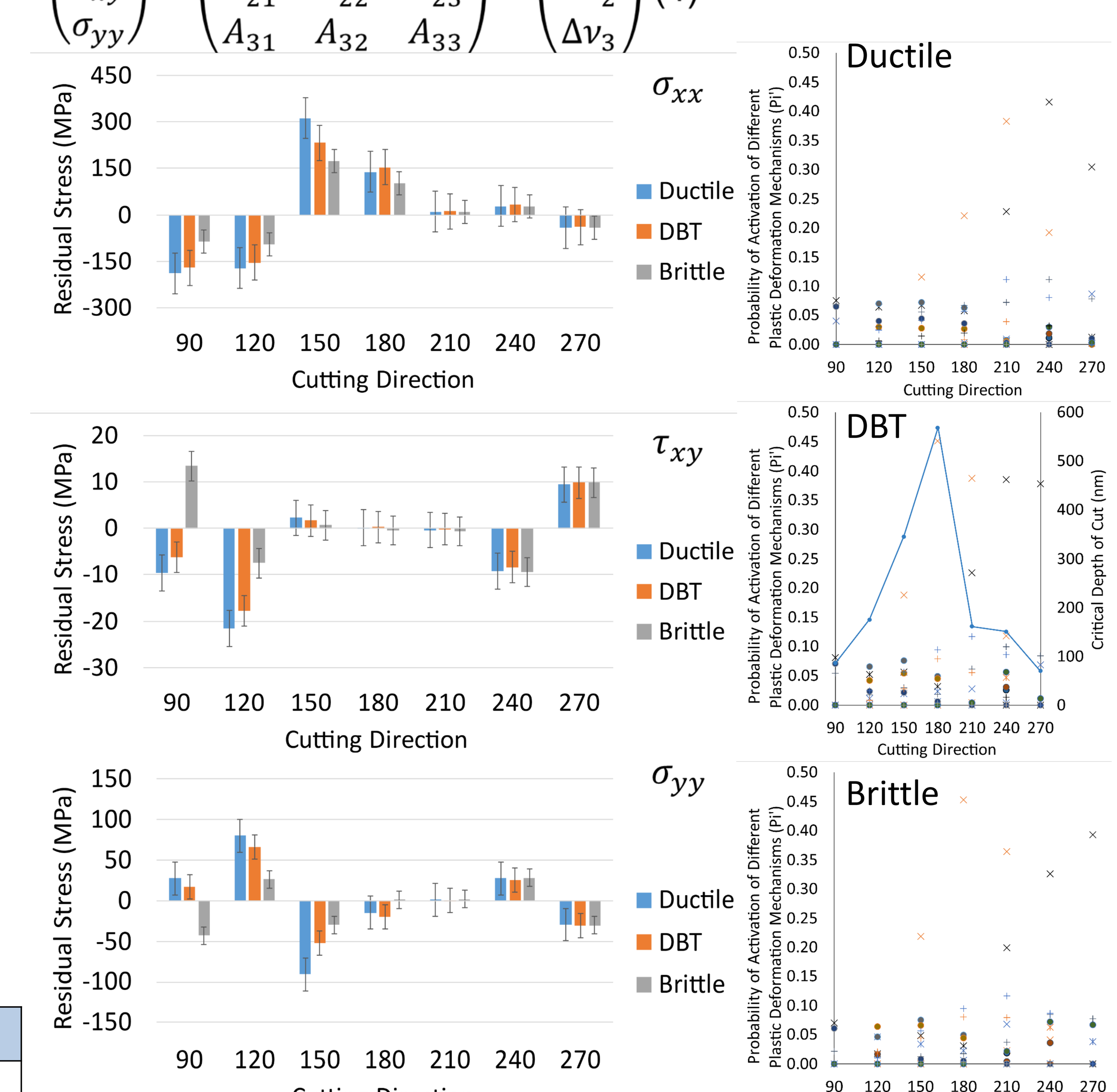

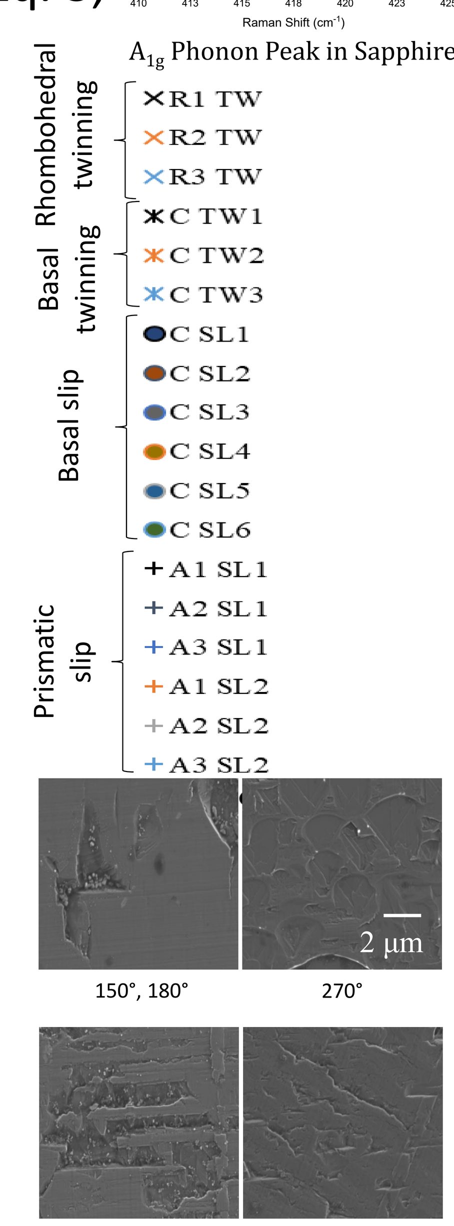

1. Residual stress magnitudes varied between -188 to 312 MPa σ_{xx} , -21 to 13 MPa τ_{xy} , and -90 to 79 MPa σ_{yy} .
2. The normal stress component along the cutting direction σ_{xx} was generally much larger than the other stress components. Across the board, residual stress in the brittle region was of lower magnitude.

Data and Results—X-ray Nanobeam

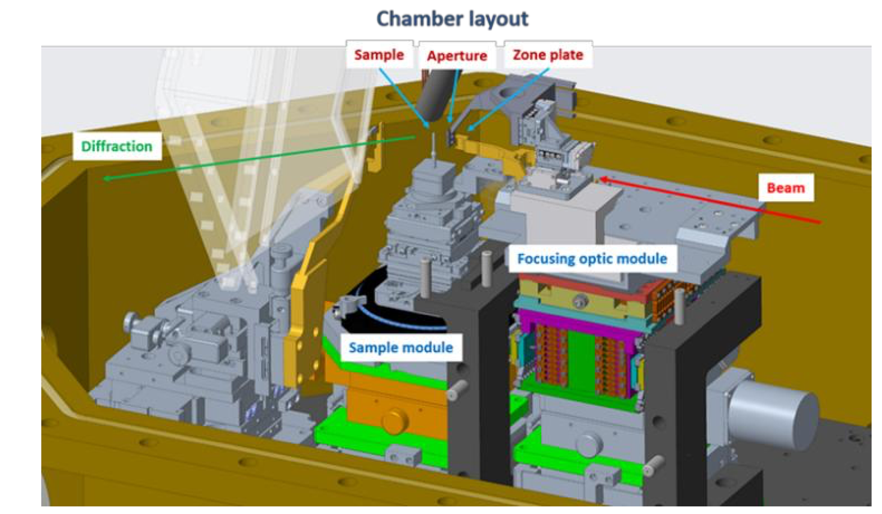

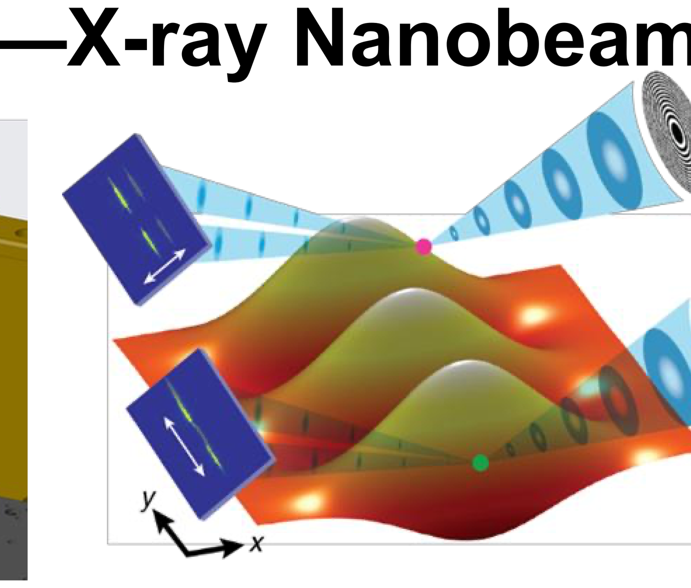

Domains of ROIs

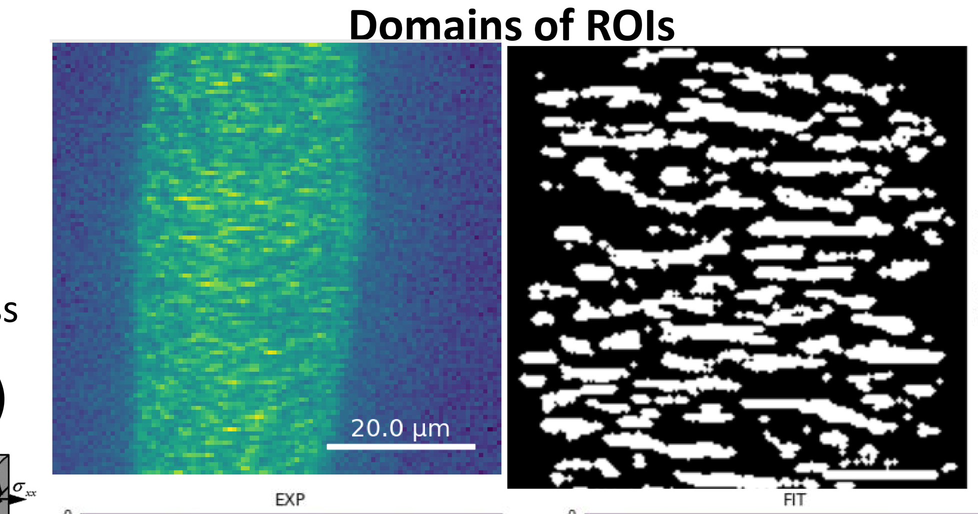

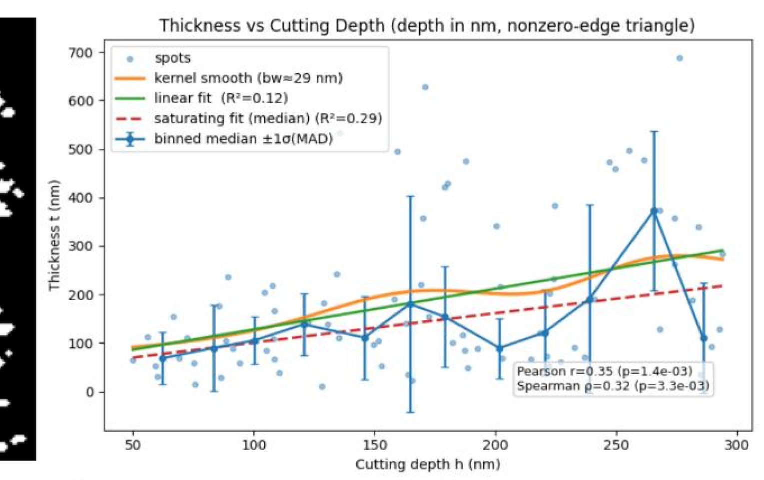

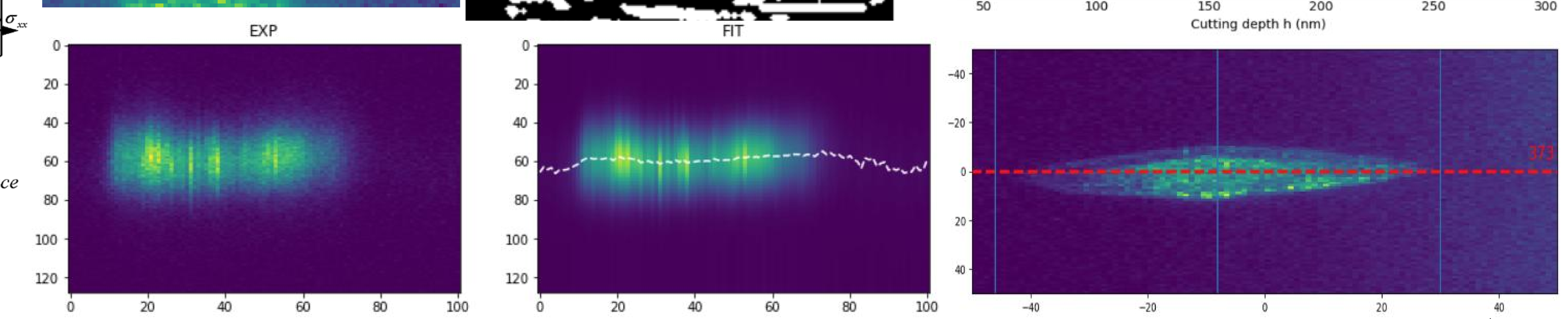

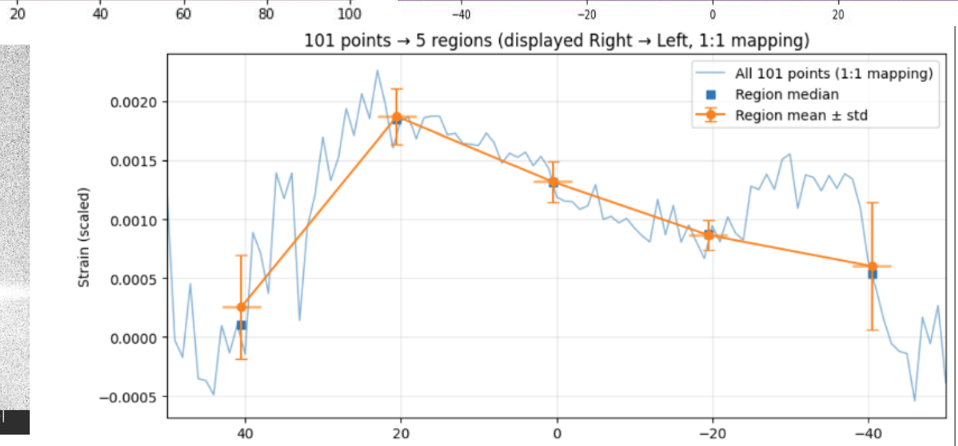

Within the ductile zone around the scratch interior 270° curves are larger, the strains decrease after the ductile region and DBT region.

Conclusion and future work:

- Expand measurements to more crystallographic orientations to study stress–deformation coupling
- Develop predictive models linking machining parameters, crystallography, and stress evolution
- Optimize machining strategies for improved surface integrity and reduced subsurface damage

References and Publications:

[1] Zhu, W., & Pezzotti, G. (2011). Raman analysis of three-dimensionally graded stress tensor components in sapphire. Journal of Applied Physics, 109(7).

[2] S. J. Whiteley, F.J. Heremans, et.al, (2019). Imaging dynamically-driven strain at the nanometer-scale using stroboscopic scanning X-ray diffraction microscopy. Nature Physics, 10:3386.

[3] Nagaraj, A., & Min, S. (2022). Effect of Crystallography on residual stresses during Ultra-precision machining of sapphire. CIRP Annuals, 71(1).

Acknowledgement

National Science Foundation under Grant No. CMMI-2339392.
FANUC Co., Japan for the donation of the ROBONANO α-0*i*B.
U.S. DOE, Office of Basic Energy Sciences, under Contract No. DE-AC02-06CH11357.